RESEARCH PAPER

Beneficial effects of C36, a novel breaker of advanced glycation endproducts cross-links, on the cardiovascular system of diabetic rats

G Cheng, L-L Wang, L Long, H-Y Liu, H Cui, W-S Qu and S Li

Beijing Institute of Pharmacology and Toxicology, Beijing, China

Background and purpose: Advanced glycation endproducts (AGE) have been implicated in the pathogenesis of diabetic complications, including diabetic cardiovascular dysfunctions. 3-benzyloxycarbonylmethyl-4-methyl-thiazol-3-ium bromide (C36), a novel AGE breaker, was investigated for its beneficial effects on the cardiovascular system of diabetic rats.
Experimental approach: The *in vitro* breaking abilities of C36 on AGE cross-links formed *in vitro* and *in vivo* were assessed. After 4 weeks' treatment with C36, cardiovascular and left ventricular functions in diabetic (streptozotocin–induced) rats were evaluated by haemodynamic studies. Effects of C36 on AGE accumulation, collagen distribution, and fibrosis-associated gene expression were also investigated by biochemical and morphological methods and reverse transcription-PCR, respectively.
Key results: *In vitro*, C36 released bovine serum albumin (BSA) from preformed AGE-BSA-collagen complexes and decreased the IgG cross-linked to red blood cell surface (RBC-IgG). *In vivo*, C36 treatment of diabetic rats resulted in a significant increase in left ventricular systolic pressure and the maximal rate of left ventricular pressure rise and pressure fall, induction in cardiac output and systemic arterial compliance, decrease of total peripheral resistance, reduction of diabetes-induced RBC-IgG content, increase of myocardial and tail tendon collagen solubility, and normalization of collagen type III/I ratio in diabetic rats. In addition, C36 treatment attenuated mRNA levels of diabetes-induced genes, including receptors for AGE, transforming growth factor β1, connective tissue growth factor, and collagen III.
Conclusions and implications: C36 was an effective breaker of AGE cross-links and had beneficial effects on the cardiovascular system of diabetic rats.
British Journal of Pharmacology (2007) **152**, 1196–1206; doi:10.1038/sj.bjp.0707533; published online 29 October 2007

Introduction

Diabetes is essentially a disorder of chronic hyperglycaemia. The most serious threat of this disease is the high mortality caused by diabetic complications, such as vascular stiffening and cardiac dysfunction. The accumulation of advanced glycation endproducts (AGEs) cross-links is one of the causes of these complications (Cooper, 2004; Zieman and Kass, 2004).

Advanced glycation endproduct comprise a heterogeneous group of complexes formed by the nonenzymatic reaction between protein amino groups and glucose or other reducing sugars through nonenzymatic glycosylation, addition, dehydration and a series of chemical rearrangement reactions over a period of time (Brownlee *et al.*, 1988a). In the 1980s, Brownlee *et al.* (1986, 1988a, b) first described the harmful consequences of AGE formation on the cardiovascular and renal systems in humans and diabetic rats. The formation of AGE and its cross-links occurs in normal ageing and is accelerated in the diabetic state. Once the AGE and its cross-links are formed, they tend to accumulate on long-lived proteins, especially structural proteins (for example, collagen and elastin), in heart and vascular tissue over time and cause tissue structure stiffness and cell stress. Finally, the myocardial and vascular systems become less flexible, which in turn contributes to the cardiovascular dysfunction observed in diabetic complications (Brownlee *et al.*, 1988a; Norton *et al.*, 1996; Avendano *et al.*, 1999; Singh *et al.*, 2001).

Correspondence: Professor L-L Wang, Beijing Institute of Pharmacology and Toxicology, 27 Taiping Road, Beijing 100850, China.
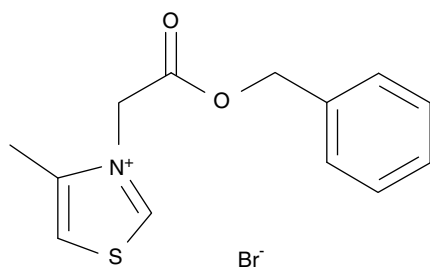E-mail: wangll@nic.bmi.ac.cn

Figure 1 The chemical structure of C36, 3-benzyloxycarbonyl-methyl-4-methyl-thiazol-3-ium bromide.

The AGE may be formed by a pathway involving reactive α-dicarbonyl intermediates (Bucala and Cerami, 1992). Vasan *et al*. (1996) were the first to investigate and validate the potential pharmacological strategy for selectively cleaving the resultant glucose-derived protein cross-links *in vitro* and *in vivo* using the first thiazolium-based AGE breaker, *N*-phenacylthiazolium bromide (PTB) (Vasan *et al*., 1996). Conceptually, this approach is novel and is independent from classical treatments (Zieman and Kass, 2004). Subsequently, ALT-711, a more stable derivative of PTB, was studied extensively and shown to reverse cardiovascular dysfunction mediated by AGE cross-links in several animal studies and eventually in clinical trials (Wolffenbuttel *et al*., 1998; Kass *et al*., 2001; Vaitkevicius *et al*., 2001). Our laboratory has been developing novel AGE breakers since 2000, based on the postulated mechanism for PTB (Vasan *et al*., 1996), the first-known thiazolium AGE breaker. Fourteen out of two hundred new compounds with potential AGE-breaking activity were chosen for their pharmacodynamics and PK/ADME (pharmacokinetic/absorption, distribution, metabolism and excretion) characteristics. One of these, a new thiazolium compound, C36 (3-benzyloxycarbonylmethyl-4-methyl-thiazol-3-ium bromide, Figure 1), was found to be as effective as ALT-711, but exhibiting lower LD_{50} in mice and no mutagenesis and teratogenesis in *ex vivo* studies (unpublished data).

In this paper, we report the efficacy of C36 as a breaker of AGE cross-links both *in vitro* and *in vivo*. The effects of C36 on cardiovascular and left ventricular (LV) functions were also investigated in rats with experimental diabetes. Furthermore, its effectiveness *in vivo* was also compared with that of the well-studied AGE breaker, ALT-711.

Methods

In vitro *tests*
Breaking activity on AGE cross-links formed in vitro. To ascertain the ability of C36 to break AGE cross-links formed *in vitro*, AGE cross-links were prepared from glycated BSA (Makita *et al*., 1992) and rat-tail-tendon collagen *in vitro*. In brief, glycated BSA was allowed to react with collagen to form AGE–BSA–collagen complexes. After incubation with test compounds, the amount of BSA remaining attached to collagen was quantified by ELISA using a rabbit polyclonal anti-BSA antibody. The detailed procedures of the assay have been described previously (Vasan *et al*., 1996; Wang *et al*.,

2004). The per cent of the breaking activity of the test compound was calculated as $100\% \times ((OD_{410}, PBS\ control) - (OD_{410}, test\ compound))/(OD_{410}, PBS\ control)$.

Breaking activity on AGE cross-links formed in vivo. IgG cross-linked to the surface of red blood cells (RBC–IgG) is an example of AGE cross-linking that is formed before other AGE cross-links *in vivo*. The content of RBC–IgG has previously been used to provide an index of protein cross-linking (Vasan *et al*., 1996; Wolffenbuttel *et al*., 1998). To test the breaking ability of C36 on AGE cross-links, red blood cells (RBCs) were isolated from diabetic rats and ELISA was performed. In brief, RBCs were washed and incubated with test compounds overnight, then washed sufficiently and transferred into the multiscreening plate (Multiscreen-HA; Millipore, Bedford, MA, USA). RBC–IgG content was determined as previously described (Cheng *et al*., 2005). The breaking activity of the test compound was expressed as the percentage decrease and calculated as $100\% \times ((OD_{410}, PBS\ control) - (OD_{410}, test\ compound))/(OD_{410}, PBS\ control)$.

In vivo *tests*
Animals and treatment. All animal care and surgical procedures were strictly in accordance with the Guide for the Care and Use of Laboratory Animals of the National Institutes of Health. Animals used in this study were supplied by Beijing Animal Center (Beijing, China), maintained on a 12-h light–dark cycle, and had free access to food and water.

Diabetes was induced by injecting streptozotocin (STZ, $70\ mg\ kg^{-1}$; i.p.) into fasting male Wistar rats at the age of 9–10 weeks. Animals with blood glucose levels $>15\ mM$ were selected and maintained for 12 weeks. After that, one set of diabetic rats was divided into five groups for haemodynamic study of the cardiovascular system: (1) diabetes control (Diabetic); (2) ALT-711 ($12.5\ mg\ kg^{-1}$) treated; (3) C36 ($12.5\ mg\ kg^{-1}$) treated; (4) C36 ($25\ mg\ kg^{-1}$) treated; and (5) C36 ($50\ mg\ kg^{-1}$) treated. Another set of diabetic rats was divided into four groups for haemodynamic studies of LV function (1) diabetes control (diabetic); (2) ALT-711 ($12.5\ mg\ kg^{-1}$) treated; (3) C36 ($12.5\ mg\ kg^{-1}$) treated; and (4) C36 ($50\ mg\ kg^{-1}$) treated. Additionally, both the sets described above were accompanied with another group of age-matched nondiabetic rats (receiving vehicle of STZ) serving as normal control (normal), respectively. ALT-711 and C36 were dissolved in distilled water before oral gavage; normal and diabetic control rats were treated with distilled water. All groups of rats were treated every day for a further 4 weeks.

Haemodynamic measurement of cardiovascular system. Details regarding the surgical procedure and haemodynamic measurements have been described elsewhere (Cheng *et al*., 2005). Briefly, after animals were anaesthetized (i.p. $50\ mg\ kg^{-1}$ pentobarbital) and ventilated with a rodent respirator (breath rate: 60–70 breaths min^{-1}, stroke volume: 0.8–1.5 ml per breath), a midsternal thoracotomy was performed, and the ascending aorta was dissected free. Then, the pressure transducer was advanced into the ascending aorta through the right carotid artery. An adapted Doppler

probe was positioned around the ascending aorta to measure phasic aortic blood flow. After the system was stabilized for 10 min, aortic blood flow and pressure were digitized at the rate of 2000 samples s^{-1} with a commercially available analog-to-digital converter (MP150WS; BIOPAC System Inc., Goleta, CA, USA) and a computer using dedicated software (Acknowledge, Version 3, BIOPAC System Inc.). All parameters were calculated on beat-to-beat basis for 30 s and then averaged. In steady-state conditions, systolic and diastolic blood pressure, cardiac output, and heart rate were measured and calculated. Total peripheral resistance (TPR) was determined as the quotient of mean arterial blood pressure and cardiac output (Levy *et al.*, 1994). Stroke volume was calculated as the quotient of cardiac output and heart rate. Systemic arterial compliance (SAC) was calculated as the quotient of stroke volume and pulse pressure (Yin *et al.*, 1983).

Haemodynamic measurement of left ventricle. The procedure was described in our previous report (Cheng *et al.*, 2005). In brief, a fluid-filled catheter was introduced through the right carotid artery into the LV of anaesthetized rats. Tracings of LV pressure were digitized at a rate of 2000 samples s^{-1} with a commercially available analogue to digital converter and a computer using dedicated software. The maximal rate of LV pressure rise (pos dP/dT_{max}) and pressure fall (neg dP/dT_{max}) were calculated from the digitized LV pressure recording.

RBC–IgG content assay. Before performing the haemo-dynamic measurements of the cardiovascular system, hepar-inized RBCs were collected and RBC–IgG was determined as previously described (Cheng *et al.*, 2005). The content of RBC–IgG was expressed as OD_{410}.

Collagen solubility assay. The presence of AGE cross-links has been proposed to contribute to the increased insolubility and resistance of collagen to enzymatic and chemical digestion (Kochakian *et al.*, 1996). The solubility of tail-tendon collagen was measured as previously described (Cheng *et al.*, 2005). To assess myocardial collagen solubility (Kochakian *et al.*, 1996; Candido *et al.*, 2003), aliquots of LV were digested with 1 ml of 200 µg ml^{-1} pepsin in 0.5 M acetic acid at 37 °C. After 2- and 24-h digestion, respectively, the supernatant was removed. The conditions for pepsin diges-tion were chosen, based on preliminary studies, to be adequate to cause significant solubilization of the unmodi-fied heart collagen after 2 h and to cause solubilization of greater than 98% of the heart sample after 24 h (Candido *et al.*, 2003). Thus, the total recoverable collagen was defined as the collagen concentration after 24 h of pepsin digestion. Myocardial collagen solubility was expressed as the percen-tage of the collagen concentration after 2 h of pepsin digestion in relation to the total recoverable collagen.

Assay for AGE content of LV and aorta. An increase of AGE as reflected by collagen-associated fluorescence has been docu-mented in experimental and human diabetes (Brownlee *et al.*, 1986, 1988a). AGE contents were determined by collagen-associated fluorescence by a method previously described (Monnier *et al.*, 1984; Soulis-Liparota *et al.*, 1991).

The collagen-associated fluorescence was determined using enzyme-digested samples at 370-nm excitation and 440-nm emission with Tecan fluorimeter (model GENios Pro). AGE contents of LV and aorta were determined by expression as arbitrary units (FAU) of collagen-specific fluorescence per microgram collagen (FAU µg per collagen).

Morphological observation of collagen distribution in aortic media wall. A 2- to 3-cm segment of the descending thoracic aorta was fixed in 10% formalin and embedded in paraffin for morphological study. Sections (7 µm) of aorta were stained with picrosirius red (Direct Red 80, Aldrich, St Louis, MO, USA, in aqueous picric acid) for 4 h. The ratio of type III/I collagen in the aortic media wall was measured by polarizing light microscopy (Nikon, E600POL), according to previously pub-lished methods (Junqueira *et al.*, 1978; Whittaker *et al.*, 1994).

Reverse transcription–PCR. The total RNA from LV and aorta were isolated using Trizol RNA preparation kit (GIBCO-BRL, Grand Island, NY, USA) following the manufacturer's recommended procedures. For reverse transcription (RT)– PCR analysis of gene expression of collagen I, collagen III, transforming growth factor-β1 (TGF-β1), connective tissue growth factor (CTGF) and receptor for AGE (RAGE), total RNA was reverse transcribed and subsequently amplified by PCR using the RNA PCR Kit Ver. 1.1 (TaKaRa Biotechnology Co. Ltd, Dalian, China). Primers for PCR are shown in Table 1. The PCR conditions were as follows: after an initial denaturation for 2 min at 94 °C, PCR was performed in indicated cycles. Each cycle consisted of denaturation at 94 °C for 20 s, primer annealing at respective temperatures for 30 s (55 °C for collagen III and RAGE, 57 °C for collagen I and TGFβ1, 60 °C for CTGF), and primer extension at 72 °C for 1 min. A final 10 min extension step at 72 °C was performed. The number of cycles used (28 for collagen III and TGFβ1, 29 for CTGF and RAGE, 26 for collagen I) was predetermined to be the greatest number of cycles within the linear range. PCR product was separated by 2% agarose gel, stained with ethidium bromide and visualized under UV light with a multilmage TM light cabinet (Alpha Imager TM 2200, USA). Levels of mRNA were normalized to glyceralde-hyde-3-phosphate dehydrogenase transcript.

Statistical analysis. All results are expressed as mean ± s.e.mean. Comparisons among groups of data were made using a one-way ANOVA followed by the Dunnett's multiple comparison tests. *P*-value of <0.05 was considered statisti-cally significant.

Drugs. C36 (3-benzyloxycarbonylmethyl-4-methyl-thiazol-3-ium bromide, chemical structure shown in Figure 1) and ALT-711 (chemical structure as described previously (Bhat *et al.*, 1991) were synthesized by the Beijing Institute of Pharmacology and Toxicology and identified by nuclear magnetic resonance spectroscopy–mass spectroscopy and elemental analysis. STZ, pepsin and picrosirius red were purchased from Sigma Chemical Co. (St Louis, MO, USA). PCR primers were synthesized by TaKaRa Biotechnology Co. Ltd. All other chemicals and substances were of analytical reagent grade unless stated otherwise.

Table 1 Sequences of the primers used in the PCR measurements

Gene	Sense	Sequence	GenBank no./ref.	Product size (bp)
Collagen I	Forward	AACCTGGAGTCAGACATGGG	XM 213440	359
	Reverse	ATGCCCACTCCCTAACAGTG		
Collagen III	Forward	GTCCACGAGGTGACAAAGGT	NM 032085	388
	Reverse	TAATATGGTGAAAAGCCGCC		
TGF-β1	Forward	CTTCAGCTCCACAGAGAAGAACTGC	NM 021578	297
	Reverse	CACGATCATGTTGGACAACTGCTCC		
CTGF	Forward	GTGTGAAGACCTACCGGGCTAAGT	NM 022266	609
	Reverse	AAGCTATAATGTCCCTCCCCTGTC		
RAGE	Forward	CACGCTTCGGTCAGAGCTCA	NM 053336	513
	Reverse	ATGAGCAGAGCGGCTATTCC		
GAPDH	Forward	TCCCTCAAGATTGTCAGCAA	X02231	307
	Reverse	AGATCCACAACGGATACATT		

Abbreviations: AGE, advanced glycation endproduct; CTGF, connective tissue growth factor; GAPDH, glyceraldehyde-3-phosphate dehydrogenase; RAGE, receptor for AGE; TGF-β1, transforming growth factor-β1.

Results

Breaking activity in vitro
As shown in Figure 2, incubation with either C36 or ALT-711, over a range of concentrations, released BSA from preformed glycated-BSA–collagen complexes. However, C36 was more effective than ALT-711 *in vitro,* at the higher concentrations used (Figure 2).

Figure 3 illustrates the effects of incubation *in vitro* with C36 or ALT-711 on AGE cross-links formed *in vivo,* using RBCs from diabetic rats in which IgG is linked to the RBC surface (RBC–IgG). After overnight incubation with either C36 or ALT-711, there was less IgG linked to the surface of the cells. Here also, C36 was more effective at lower concentrations, than ALT-711.

Assay of C36 actions in vivo
We first analysed the effects of C36 on cardiovascular functions in diabetic rats (Table 2). Compared with normal nondiabetic control rats, the diabetic rats exhibited lower body weight, heart rate, cardiac output and SAC. Diabetic rats also had higher TPR and TPR index. As shown in Table 2, treatment with ALT-711 or C36 for 4 weeks resulted in significant increases in cardiac output and cardiac index, reduction of TPR and TPR index, and increase of stroke volume and SAC, as compared to untreated diabetic rats. Further, C36 increased SAC in a dose-dependent fashion (Table 2).

We next sought to evaluate the effect of C36 on LV function. We found that both contractile functions, such as left ventricular systolic pressure (LVSP) and pos dP/dT_{max}, and relaxant functions, such as neg dP/dT_{max}, were decreased significantly in the diabetic group, compared to normal rats (Table 3). However, treatment with either C36 (12.5, 50 mg kg^{-1}) or ALT-711 (12.5 mg kg^{-1}) for 4 weeks resulted in a significant increase in all of these three
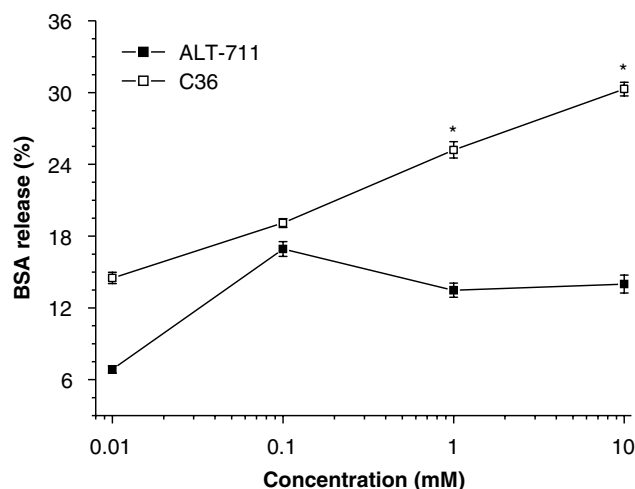

Figure 2 Breaking of advanced glycation endproduct (AGE) cross-links *in vitro*. Preformed AGE–BSA–collagen complexes were incubated with C36 or ALT-711 and the subsequent release of BSA assayed by ELISA. Both C36 and ALT-711 increased the release of BSA from the AGE–BSA–collagen complex, but C36 was more effective at the higher concentrations used. All values are given as mean ± s.e.mean ($n = 6$). *$P < 0.05$ vs corresponding value of ALT-711. C36, 3-benzyloxycarbonylmethyl-4-methyl-thiazol-3-ium bromide.

parameters (Table 3) as compared to untreated diabetic rats, without changing body weight or blood glucose levels.

Effects of C36 on RBC–IgG content
IgG cross-linked to red blood cell surface content usually represents the extent of AGE cross-linking to the surface of RBC in diabetes. To assess if treatment with C36 *in vivo* could reverse this process, the RBC–IgG content in six groups of animals were measured. As shown in Figure 4, diabetic rats have significantly higher RBC–IgG content than that in
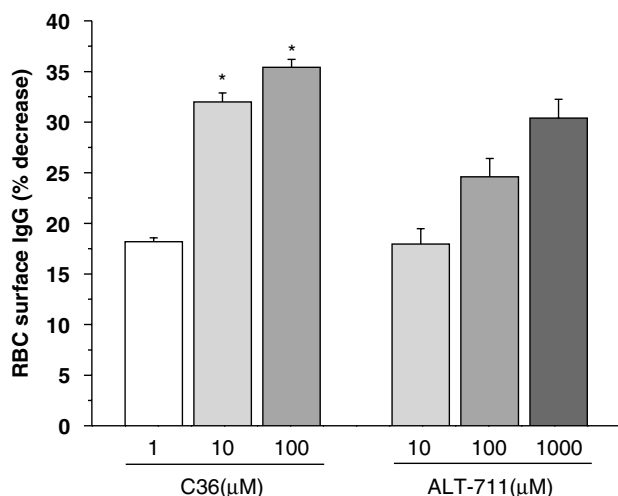
Figure 3 Breaking of advanced glycation endproduct (AGE) cross-links *in vitro*. AGE cross-links were formed *in vivo* as IgG cross-linked to the surface of red blood cells (RBC–IgG). RBCs from diabetic rats were incubated overnight with C36 or ALT-711 and release of IgG into the supernatant measured. C36 increased IgG release in a concentration-dependent manner. All values are given as mean ± s.e.mean ($n = 6$). *$P < 0.05$ vs corresponding value of ALT-711. C36, 3-benzyloxycarbonylmethyl-4-methyl-thiazol-3-ium bromide.

normal rats. However, treatment with either C36 (25, 50 mg kg^{-1}) or ALT-711 (12.5 mg kg^{-1}) for 4 weeks resulted in a significant decrease in RBC–IgG content as compared to diabetic rats. The effects of C36 appeared to be dose-dependent (Figure 4).

Effects of C36 on collagen solubility

Compared with normal rats, the solubility of tail-tendon collagen in the diabetic rats was significantly decreased (Figure 5). After *in vivo* treatment with C36 or ALT-711, the collagen solubility was increased significantly (Figure 5), but this effect was significantly less for ALT-711 (12.5 mg kg^{-1}) than that of C36 (50 mg kg^{-1}; Figure 5). The solubility of myocardial LV collagen was also decreased in diabetic rats but increased significantly after 4 weeks of treatment with either C36 (50 mg kg^{-1}) or ALT-711 (12.5 mg kg^{-1}).

Effects of C36 on AGE contents in LV myocardium and aorta

We found that the accumulation of AGE in myocardial and aorta collagen, as assessed by collagen-associated fluorescence were significantly increased in diabetic rats compared

Table 2 Effects of treatment with C36 or ALT-711 for 4 weeks on haemodynamic measurements in diabetic rats

		Normal	*Diabetic*	*ALT-711*		*C36*	
Dosage	mg kg^{-1}			12.5	12.5	25	50
Blood glucose	mM	4.1 ± 0.03	26.8 ± 0.32[##]	27.4 ± 0.34	27.1 ± 0.30	26.1 ± 0.40	27.4 ± 0.28
Body weight	g	469.9 ± 1.6	294.9 ± 2.6[##]	317.4 ± 3.6	290.8 ± 3.1	302.3 ± 2.4	307.5 ± 3.3
Systolic BP	mm Hg	121.4 ± 2.0	123.2 ± 1.8	121.5 ± 2.2	119.1 ± 2.0	116.0 ± 0.8	108.7 ± 1.3
Diastolic BP	mm Hg	100.6 ± 1.8	92.7 ± 1.9	93.2 ± 2.6	88.5 ± 2.2	88.5 ± 1.3	83.8 ± 1.6
Mean BP	mm Hg	107.5 ± 1.8	102.9 ± 1.8	102.6 ± 2.4	98.7 ± 2.1	97.7 ± 1.1	92.1 ± 1.5
Pulse BP	mm Hg	20.8 ± 0.2	30.6 ± 0.7[##]	28.3 ± 0.6	30.7 ± 1.1	27.5 ± 0.7	25.7 ± 0.4
Heart rate	beats min^{-1}	351.9 ± 3.1	312 ± 4.6[#]	319.3 ± 4.2	303.3 ± 5.6	309.7 ± 2.3	293 ± 2.1
Cardiac output	ml min^{-1}	103.9 ± 1.0	66.8 ± 0.5[##]	80.0 ± 0.9**	74.4 ± 0.8*	78.3 ± 0.7**	82.2 ± 0.8**
Cardiac index	ml min^{-1} cm^{-2}	0.188 ± 0.002	0.166 ± 0.001[#]	0.189 ± 0.002**	0.186 ± 0.001*	0.191 ± 0.002**	0.198 ± 0.002**
TPR	10^3 dyne s cm^{-5}	83.5 ± 1.6	123.3 ± 2.0[##]	102.6 ± 2.3*	107.3 ± 2.6	101.1 ± 1.9*	90.7 ± 1.8**
TPR index	dyne s cm^{-3}	128.9 ± 4.9	305.0 ± 4.5[##]	240.8 ± 4.4**	269.8 ± 6.7	246.3 ± 4.3*	219.8 ± 4.8**
Stroke volume	ml per beat	0.297 ± 0.004	0.218 ± 0.004[##]	0.254 ± 0.003*	0.252 ± 0.004	0.255 ± 0.004*	0.282 ± 0.003**
SAC	10^{-3} ml per mm Hg	14.6 ± 0.2	7.3 ± 0.1[##]	9.3 ± 0.2*	8.8 ± 0.2	9.8 ± 0.2**	11.4 ± 0.1**○

Abbreviations: Cardiac index, cardiac output corrected for body surface area; DBP, diastolic blood pressure; SAC, systemic arterial compliance; SBP, systolic blood pressure; TPR, total peripheral resistance; TPR index, TPR corrected for body surface area.
All values are given as mean ± s.e.mean ($n = 10$).
[#]$P < 0.05$, [##]$P < 0.01$ vs normal control, *$P < 0.05$, **$P < 0.01$ vs diabetic, ○$P < 0.05$ vs C36 12.5 mg kg^{-1}.

Table 3 Effects of treatment with C36 or ALT-711 on LV function in diabetic rats

		Normal	*Diabetic*	*ALT-711*	*C36*	
Dosage	mg kg^{-1}			12.5	12.5	50
Blood glucose	mM	4.2 ± 0.1	26.4 ± 0.2[##]	27.4 ± 0.4	27.1 ± 0.2	27.1 ± 0.4
Body weight	g	479 ± 1.4	307 ± 2.3[##]	289 ± 2.6	298 ± 2.1	304 ± 1.6
Heart rate	beats min^{-1}	354 ± 3.1	314 ± 1.8[##]	341 ± 3.9*	310 ± 1.3	333 ± 1.6*
LVSP	mm Hg	146.7 ± 1.6	116.9 ± 0.9[##]	130 ± 1.7*	128.7 ± 1.0*	136.3 ± 0.6**
pos dP/dT_{max}	mm Hg s^{-1}	3731.1 ± 11.1	2928.6 ± 27.5[##]	3489 ± 36.9**	3265.7 ± 23.0**	3469.3 ± 15.6**
neg dP/dT_{max}	mm Hg s^{-1}	3440.7 ± 20.2	2626.3 ± 35.1[##]	3221 ± 41.0**	2927.9 ± 24.4*	3252.3 ± 11.9**

Abbreviations: LVSP, left ventricular systolic pressure; neg dP/dT_{max}, maximal rate of LV pressure fall; pos dP/dT_{max}, maximal rate of LV pressure rise.
All values are given as mean ± s.e.mean ($n = 10$).
[#]$P < 0.05$, [##]$P < 0.01$ vs normal control, *$P < 0.05$, **$P < 0.01$ vs diabetic.
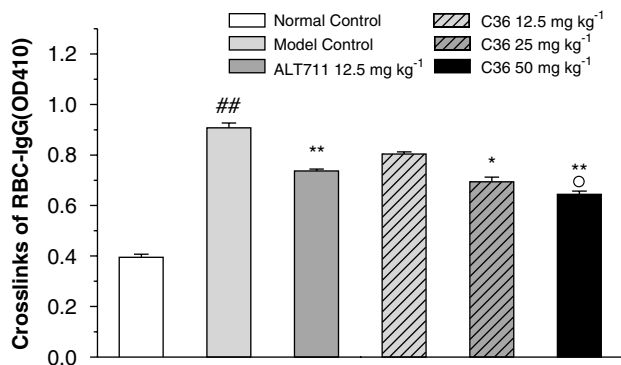
Figure 4 Effects of treatment *in vivo* with C36 or ALT-711 on IgG cross-linked to the RBC surface in diabetic rats. All values are given as mean ± s.e.mean ($n = 8$). [##]$P < 0.01$ vs nondiabetic normal control, *$P < 0.05$, **$P < 0.01$ vs untreated diabetic (model control) and °$P < 0.05$ vs C36 (12.5 mg kg^{-1}). C36, 3-benzyloxycarbonylmethyl-4-methyl-thiazol-3-ium bromide.
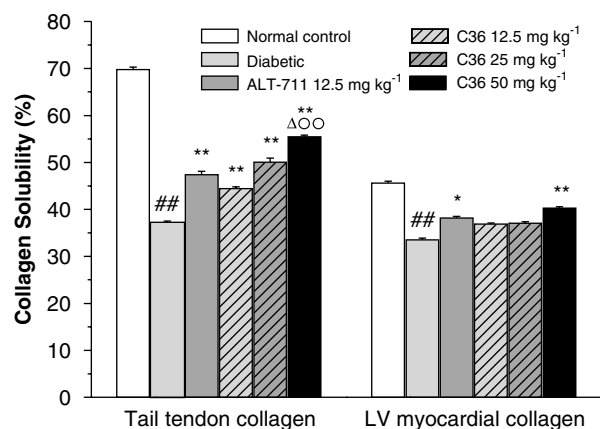

Figure 5 Effects of treatment *in vivo* with C36 or ALT-711 on the solubility of tail-tendon collagen and of LV myocardial collagen, in diabetic rats. All values are given as mean ± s.e.mean ($n = 10$). [##]$P < 0.01$ vs nondiabetic normal control, *$P < 0.05$, **$P < 0.01$ vs diabetic, [Δ]$P < 0.05$ vs ALT-711 and °°$P < 0.01$ vs C36 12.5 mg kg^{-1}. C36, 3-benzyloxycarbonylmethyl-4-methyl-thiazol-3-ium bromide.

with normal controls (Figure 6). However, after treatment *in vivo* with C36 (12.5, 25 and 50 mg kg^{-1}), the LV myocardial and aorta fluorescence were significantly decreased in a dose-dependent fashion, as compared to untreated diabetic rats (Figure 6). Similarly, ALT-711 (12.5 mg kg^{-1}) treatment resulted in a significant decrease of fluorescence in the LV myocardium and aorta, as compared to diabetic rats.

Effects of C36 on the ratio of collagen type I and type III in aortic media wall

After staining with picrosirius red, different types of collagen in the aortic media wall were distinguished by polarizing light microscopy, where type I collagen appeared to be yellow or yellow-red, and type III collagen, green (Figure 7). In this set of experiments, the type III/I collagen ratio of the aortic media wall tended to increase in diabetic rats (Figure 7b). Treatment of diabetic rats with C36 (50 mg kg^{-1}) or ALT-711 (12.5 mg kg^{-1}) reversed this change (Figures 7c and d, respectively).
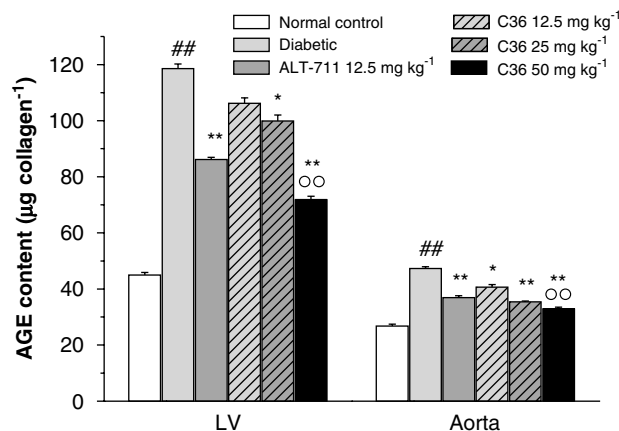

Figure 6 Effects of treatment *in vivo* with C36 or ALT-711 on the advanced glycation endproduct (AGE)-collagen content in LV and aorta in diabetic rats. Fluorescence corrected for collagen (as FAU µg per collagen). All values are given as mean ± s.e.mean ($n = 8$). [##]$P < 0.01$ vs nondiabetic normal control, *$P < 0.05$, **$P < 0.01$ vs diabetic and °°$P < 0.01$ vs C36 12.5 mg kg^{-1}. C36, 3-benzyloxy-carbonylmethyl-4-methyl-thiazol-3-ium bromide.

RT–PCR results

Receptors for AGE have been identified, and via receptor-dependent mechanisms, AGE induction of cytokines and growth factors has been proposed to contribute to diabetic complications (Cooper, 2001; Candido *et al.*, 2003). To investigation whether C36 treatment can reverse these processes, we measured the expression of some relevant genes in aortas and LV of diabetic rats. Compared with normal rats, the gene expression of RAGE, TGF-β1, CTGF and collagen III were upregulated in diabetic aortas. C36 and ALT-711 prevented the increase in expression of these genes, and no significant differences were observed when C36 and ALT-711 treatment were compared (Figure 8). Changes in the expression of these genes in aorta paralleled those seen in LV myocardium (Figure 9).

Discussion

The present study shows that C36, a novel breaker of AGE cross-links, could break these links both *in vitro* and *in vivo*, thus improving the functions of the cardiovascular system of diabetic rats.

Advanced glycation endproduct cross-links are permanent and irreversible complexes formed when glucoses bind to the target proteins. These are usually housekeeping proteins including collagen and elastin. AGE cross-links accumulate in diabetic patients and animals and cause diabetic cardio-vascular complications (Singh *et al.*, 2001). Therefore, the breakdown of these complexes provides a potential treatment for such diabetic complications.

In this study, we evaluated C36 as an AGE cross-links breaker and found that C36 could cleave these cross-links very effectively *in vitro*. To confirm this activity of C36 *in vivo*, several tests were performed in STZ-induced diabetic rats. Treatment with C36 for 4 weeks resulted in a significant increase in LVSP, pos dP/dT_{max} and neg dP/dT_{max}; and an
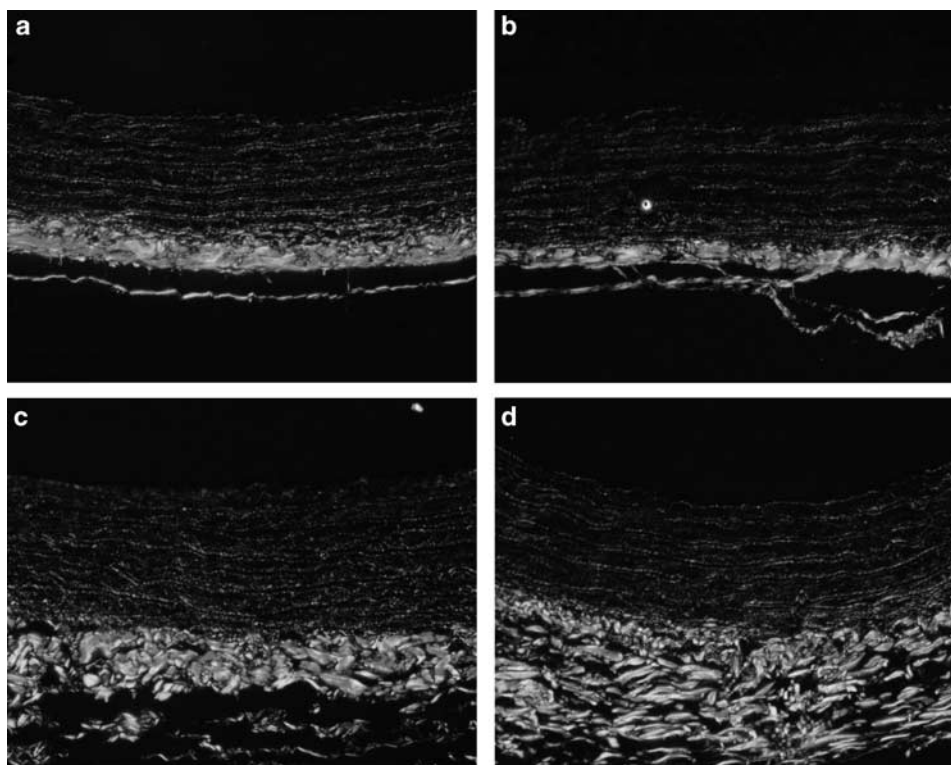
Figure 7 Picrosirius red staining for the distribution of collagen between types I and III in descending thoracic aorta from normal control rats (**a**), diabetic (**b**), C36-treated (**c**) and ALT-711-treated (**d**) rats. Type I collagen appears yellow or yellow-red, while type III collagen appears green. Magnification $\times 200$.

increase of cardiac output and SAC; accompanied by decreased TPR. Furthermore, C36 reduced the diabetes-induced RBC–IgG content, increased myocardial and tail-tendon collagen solubility, and normalized the collagen type III/I ratio in diabetic rats. Finally, C36 treatment attenuated mRNA levels of diabetes-induced genes, including RAGE, TGF-β1, CTGF and collagen III in aorta and myocardium.

Structural matrix proteins such as collagen and elastin play an integral role in the maintenance of cardiovascular elasticity function and vascular wall integrity (Bruel and Oxlund, 1996). It is believed that formation and accumulation of AGE cross-links in matrix proteins result in biomechanically rigid structures and tissue stiffness, eventually impairing the normal functions of contractile organs (Brownlee *et al*., 1988a; Avendano *et al*., 1999). In this study, we found that diabetes not only led to significant accumulation of AGE cross-links in aorta and myocardium, but also promoted tissue stiffness and dysfunction. However, after C36 treatment *in vivo*, the above parameters were restored significantly. The increase of SAC and the decrease of TPR indicated that the stiffness of the aorta was reduced to the levels comparable to those observed in normal control rats. Both the diastolic functions of LV, such as neg dP/dT_{max}, and the contractile functions, such as LVSP and pos dP/dT_{max}, were also improved significantly. These results further substantiate the effectiveness of C36 on the dysfunction in the cardiovascular system in diabetic rats.

It is widely accepted that pathological actions of AGE are mediated through two mechanisms, one receptor independent and the other, receptor dependent. The first is considered particularly relevant to arterial and myocardial stiffening through overaccumulation of AGE related to the extracellular matrix. The latter tend to be more important in the genesis and exacerbation of macrovascular and cardiac diseases through various cellular stress challenges (Zhou *et al*., 2003). RAGE acts as a signal transduction receptor for AGE. RAGE–AGE interaction activates multiple intracellular signalling pathways, including P21/RAS, MAP kinase p38, CDC42/RAC, NAD(P)H oxidase/reactive oxygen species and nuclear transcription factors, such as NF-κB. In contrast to many other receptor systems, the RAGE–AGE interaction is thought to upregulate RAGE expression and to amplify the inflammatory and oxidative damage cascade at the local site of tissue damage (Schmidt *et al*., 2001). Like AGE, an increased level of RAGE had been found in cardiac and renal tissue in diabetes (Brett *et al*., 1993). ALT-711 treatment reduced cardiac and renal AGE levels and prevented the increase in RAGE expression (Candido *et al*., 2003; Coughlan *et al*., 2007). As expected, diabetic rats exhibited increased AGE and RAGE expression in LV and thoracic aorta, which were reduced significantly by C36 treatment in this study.

In diabetes, fibrosis is also an important pathological cause of end-organ function impairment and development of complications. Recently, several studies have shown that the upregulation of profibrotic cytokines and abnormal distribution of extracellular matrices are associated with the increased AGE and RAGE levels in diabetes (Yan *et al*., 1994; Throckmorton *et al*., 1995; Stern *et al*., 2002; Candido
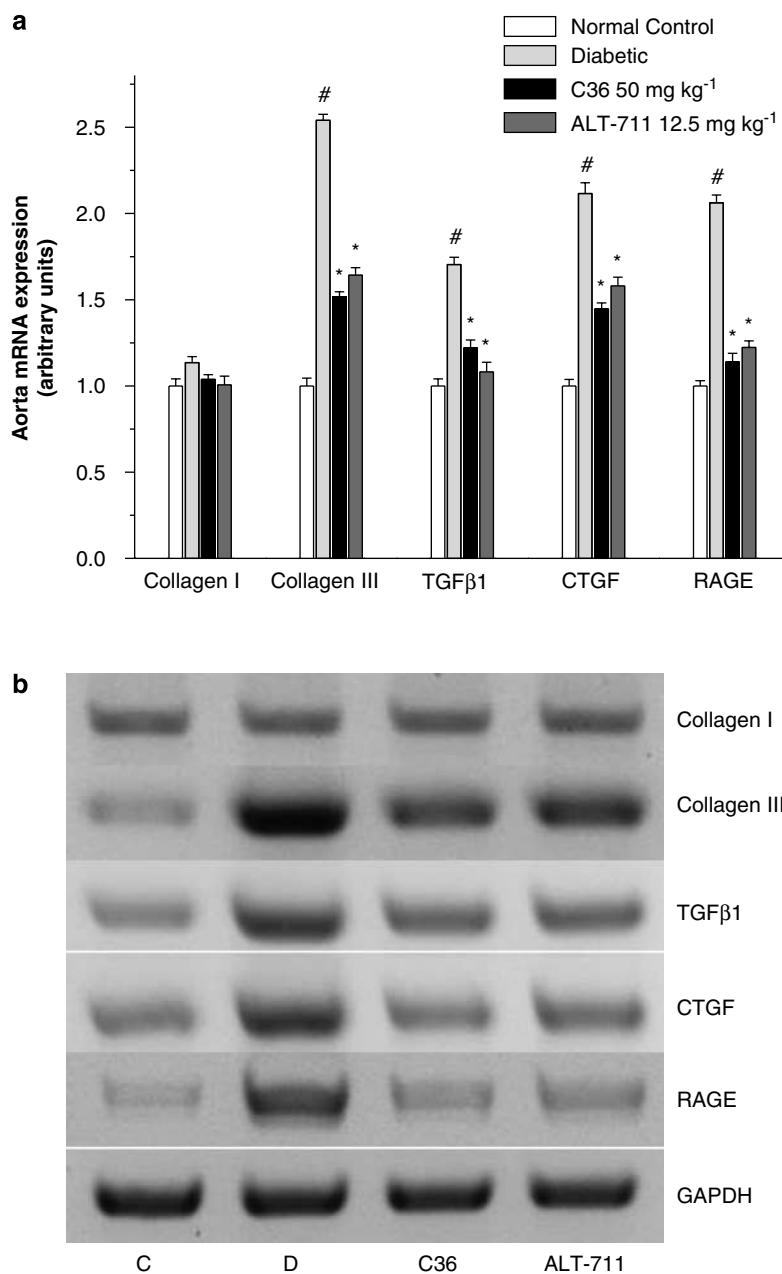
Figure 8 (a) Expression of genes for collagen I, collagen III, transforming growth factor-β1 (TGF-β1), connective tissue growth factor (CTGF) and receptor for AGE (RAGE), assayed by reverse transcription (RT)–PCR, in aorta from normal control and untreated, C36-treated, ALT-treated diabetic rats. Gene expression was normalized to the glyceraldehyde-3-phosphate dehydrogenase (GAPDH) mRNA level and expressed relative to the normal control group, which was arbitrarily designated as 1. All values are given as mean ± s.e.mean ($n = 5$). $^\#P < 0.01$ vs nondiabetic normal control, $^*P < 0.01$ vs diabetic. (b) Shows a representative gel. Lanes: C (normal control), D (diabetic), C36 (C36 50 mg kg^{-1} treatment), ALT-711 (ALT-711 12.5 mg kg^{-1} treatment). AGE, advanced glycation endproduct; C36, 3-benzyloxycarbonylmethyl-4-methyl-thiazol-3-ium bromide.

et al., 2003). Although the precise mechanisms are not yet clear, RAGE-dependent pathways are believed to be involved in the fibrosis-related actions (Throckmorton et al., 1995). TGF-β1, a potent profibrotic growth factor leading to extracellular matrix accumulation and fibrosis, was elevated in diabetes (Twigg et al., 2002a; Candido et al., 2003; Zhou et al., 2004). CTGF, a recently identified peptide that acts as a downstream mediator of TGF-β1-induced fibrosis, has also been implicated in diabetes-induced renal fibrosis and

shown to be specifically stimulated by AGE in a range of cell types, including human dermal fibroblasts and mesangial cells in vitro (Murphy et al., 1999; Twigg et al., 2002b). In this study, we found that diabetes not only increased the gene expression of RAGE, but also increased the gene expression of TGF-β1 and CTGF in LV and aorta. Those results are in agreement with that observed in the study of Candido et al. (2003). However, C36 treatment prevented the increase in RAGE, TGFβ1, CTGF in LV and in aorta.
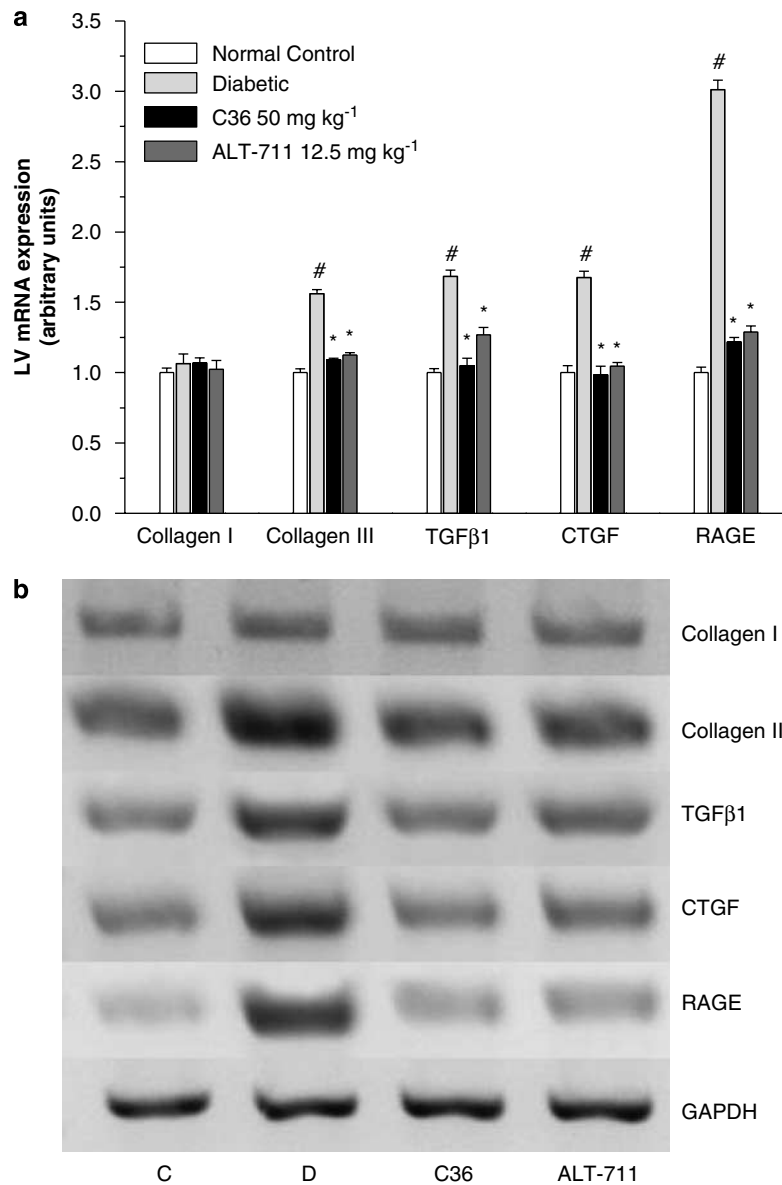
Figure 9 (a) Expression of genes for collagen I, collagen III, transforming growth factor-β1 (TGF-β1), connective tissue growth factor (CTGF) and receptor for AGE (RAGE), assayed by reverse transcription (RT)–PCR, in LV from normal control and untreated, C36-treated, ALT-treated diabetic rats. Gene expression was normalized to the glyceraldehyde-3-phosphate dehydrogenase (GAPDH) mRNA level and expressed relative to the normal control group, which was arbitrarily designated as 1. All values are given as mean ± s.e.mean ($n = 5$). [#]$P < 0.01$ vs nondiabetic normal control, [*]$P < 0.01$ vs diabetic. (b) represents gel figure. Lanes: C (normal control), D (diabetic), C36 (C36 50 mg kg^{-1} treatment), ALT-711 (ALT-711 12.5 mg kg^{-1} treatment). AGE, advanced glycation endproduct; C36, 3-benzyloxycarbonylmethyl-4-methyl-thiazol-3-ium bromide.

Collagen, especially the types III and I collagen, are integral components of structural protein in cardiovascular tissue. The type I collagen is present as thicker fibres distributed in the elastic laminae and contributes significantly to the tensile strength of the vessel wall. Type III collagen is present as thin fibres interlaced with the thicker fibres forming a fibrous network which, together with the elastic laminae, allows the aorta to regain its shape by recoiling from pressure–volume deformation. It has been proposed to contribute to the elastic properties of the vessel wall (Bruel and Oxlund, 1996). The earlier studies have generally shown an association between increased collagen type III and/or III/I ratio with the accumulation of AGE cross-links in diabetic patients and rats (Shimizu et al., 1993; Bruel and Oxlund, 1996). In this study, STZ-induced diabetic rats with 16 weeks duration of diabetes exhibited a marked increase of collagen type III/I ratio as assessed by picrosirius red staining and by RT–PCR of arterial collagen distribution and gene expression. However, there were no significant changes in type I collagen protein and gene expression in the diabetic aorta. Therefore, it is more likely that an increase of type III collagen expression is the main event induced by glucose-derived cross-linking of extracellular collagen matrix. We also observed such results in myocardium that were

consistent with previous reports (Shimizu *et al.*, 1993; Candido *et al.*, 2003). As would be predicted, C36 treatment reduced the type III collagen expression and decreased the ratio of type III/I collagen. In fact, those reductions in aorta and myocardium would lead to tissue remodelling and normalization of structures and be beneficial to cardiovascular function.

It was noticed that C36 appeared to be more effective than ALT-711 (a thiazolium compound known to act as an AGE breaker) *in vitro*, but the effects of C36 *in vivo* were not significantly greater than those of ALT-711 when different C36 treatments and ALT-711 treatments were compared. This may be attributed to the different pharmacokinetics of ALT-711 and C36 *in vivo*. In our results from the *in vivo* assays, heart rate did not change significantly during treatment with C36 or ALT-711 (Table 2) as compared to the untreated diabetic group, which was consistent with previous studies on ALT-711 (Wolffenbuttel *et al.*, 1998; Cheng *et al.*, 2005). However, in LV function experiments, both ALT-711 and C36 treatments resulted in a significant increase in heart rate (Table 3). These disparate results may simply be due to differences in experimental protocols, but they remain to be clarified in future studies. Since AGE is a heterogeneous group of complexes, the exact mechanisms underlying the breaking activities of ALT-711 or PTB *in vivo* remain unclear. However, previous studies have provided *in vivo* evidence that the thiazolium class of compounds were able to retard AGE accumulation *in vivo* (Cooper *et al.*, 2000; Candido *et al.*, 2003). Another new thiazolium compound, C36 also significantly reduced AGE accumulation *in vivo* in the present study, suggesting that C36 could also specifically break AGE *in vivo*. Whether C36 remains stably linked to one partner of the original protein–protein cross-link remains to be determined. Further, whether C36 itself has any direct or acute effect on normal rats, as well, remains undetermined at present. Our studies involved the myocardium and aorta, but PTB also prevented the increase of AGE in smaller blood vessels such as the mesenteric artery and the diabetes-associated mesenteric vascular hypertrophy, through its AGE-breaking effects on preformed AGE (Cooper *et al.*, 2000), an effect that was not explored in the present study.

In summary, C36, a novel AGE cross-link breaker, has the ability to reduce AGE cross-links *in vitro* and *in vivo*, to prevent fibrosis-associated gene expression and to improve diabetes-associated cardiovascular dysfunction in rats. This provides a potential therapeutic approach for cardiovascular stiffness in diabetes.

Acknowledgements

Conflict of interest

The authors state no conflict of interest.

References

Avendano GF, Agarwal RK, Bashey RI, Lyons MM, Soni BJ, Jyothirmayi GN et al. (1999). Effects of glucose intolerance on myocardial function and collagen-linked glycation. *Diabetes* **48**: 1443–1447.

Bhat PP, Mishra BP, Bhat PN (1991). Identification and size variation of terminal fragments of sheep pox virus genome. *Indian J Exp Biol* **29**: 434–436.

Brett J, Schmidt AM, Yan SD, Zou YS, Weidman E, Pinsky D et al. (1993). Survey of the distribution of a newly characterized receptor for advanced glycation end products in tissues. *Am J Pathol* **143**: 1699–1712.

Brownlee M, Cerami A, Vlassara H (1988a). Advanced glycosylation end products in tissue and the biochemical basis of diabetic complications. *N Engl J Med* **318**: 1315–1321.

Brownlee M, Cerami A, Vlassara H (1988b). Advanced products of nonenzymatic glycosylation and the pathogenesis of diabetic vascular disease. *Diabetes Metab Rev* **4**: 437–451.

Brownlee M, Vlassara H, Kooney A, Ulrich P, Cerami A (1986). Aminoguanidine prevents diabetes-induced arterial wall protein cross-linking. *Science* **232**: 1629–1632.

Bruel A, Oxlund H (1996). Changes in biomechanical properties, composition of collagen and elastin, and advanced glycation endproducts of the rat aorta in relation to age. *Atherosclerosis* **127**: 155–165.

Bucala R, Cerami A (1992). Advanced glycosylation: chemistry, biology, and implications for diabetes and aging. *Adv Pharmacol* **23**: 1–34.

Candido R, Forbes JM, Thomas MC, Thallas V, Dean RG, Burns WC et al. (2003). A breaker of advanced glycation end products attenuates diabetes-induced myocardial structural changes. *Circ Res* **92**: 785–792.

Cheng G, Wang LL, Qu WS, Long L, Cui H, Liu HY et al. (2005). C16, a novel advanced glycation endproduct breaker, restores cardiovascular dysfunction in experimental diabetic rats. *Acta Pharmacol Sin* **26**: 1460–1466.

Cooper ME (2001). Interaction of metabolic and haemodynamic factors in mediating experimental diabetic nephropathy. *Diabetologia* **44**: 1957–1972.

Cooper ME (2004). Importance of advanced glycation end products in diabetes-associated cardiovascular and renal disease. *Am J Hypertens* **17**: 31S–38S.

Cooper ME, Thallas V, Forbes J, Scalbert E, Sastra S, Darby I et al. (2000). The cross-link breaker, N-phenacylthiazolium bromide prevents vascular advanced glycation end-product accumulation. *Diabetologia* **43**: 660–664.

Coughlan MT, Thallas-Bonke V, Pete J, Long DM, Gasser A, Tong DC et al. (2007). Combination therapy with the advanced glycation end product cross-link breaker, alagebrium, and angiotensin converting enzyme inhibitors in diabetes: synergy or redundancy? *Endocrinology* **148**: 886–895.

Junqueira LC, Cossermelli W, Brentani R (1978). Differential staining of collagens type I, II and III by Sirius Red and polarization microscopy. *Arch Histol Jpn* **41**: 267–274.

Kass DA, Shapiro EP, Kawaguchi M, Capriotti AR, Scuteri A, deGroof RC et al. (2001). Improved arterial compliance by a novel advanced glycation end-product crosslink breaker. *Circulation* **104**: 1464–1470.

Kochakian M, Manjula BN, Egan JJ (1996). Chronic dosing with aminoguanidine and novel advanced glycosylation end product-formation inhibitors ameliorates cross-linking of tail tendon collagen in STZ-induced diabetic rats. *Diabetes* **45**: 1694–1700.

Levy BI, Duriez M, Phillippe M, Poitevin P, Michel JB (1994). Effect of chronic dihydropyridine (isradipine) on the large arterial walls of spontaneously hypertensive rats. *Circulation* **90**: 3024–3033.

Makita Z, Vlassara H, Cerami A, Bucala R (1992). Immunochemical detection of advanced glycosylation end products *in vivo*. *J Biol Chem* **267**: 5133–5138.

Monnier VM, Kohn RR, Cerami A (1984). Accelerated age-related browning of human collagen in diabetes mellitus. *Proc Natl Acad Sci USA* **81**: 583–587.

Murphy M, Godson C, Cannon S, Kato S, Mackenzie HS, Martin F et al. (1999). Suppression subtractive hybridization identifies high

glucose levels as a stimulus for expression of connective tissue growth factor and other genes in human mesangial cells. *J Biol Chem* **274**: 5830–5834.

Norton GR, Candy G, Woodiwiss AJ (1996). Aminoguanidine prevents the decreased myocardial compliance produced by streptozotocin-induced diabetes mellitus in rats. *Circulation* **93**: 1905–1912.

Schmidt AM, Yan SD, Yan SF, Stern DM (2001). The multiligand receptor RAGE as a progression factor amplifying immune and inflammatory responses. *J Clin Invest* **108**: 949–955.

Shimizu M, Umeda K, Sugihara N, Yoshio H, Ino H, Takeda R *et al.* (1993). Collagen remodelling in myocardia of patients with diabetes. *J Clin Pathol* **46**: 32–36.

Singh R, Barden A, Mori T, Beilin L (2001). Advanced glycation end-products: a review. *Diabetologia* **44**: 129–146.

Soulis-Liparota T, Cooper M, Papazoglou D, Clarke B, Jerums G (1991). Retardation by aminoguanidine of development of albuminuria, mesangial expansion, and tissue fluorescence in streptozocin-induced diabetic rat. *Diabetes* **40**: 1328–1334.

Stern D, Yan SD, Yan SF, Schmidt AM (2002). Receptor for advanced glycation endproducts: a multiligand receptor magnifying cell stress in diverse pathologic settings. *Adv Drug Deliv Rev* **54**: 1615–1625.

Throckmorton DC, Brogden AP, Min B, Rasmussen H, Kashgarian M (1995). PDGF and TGF-beta mediate collagen production by mesangial cells exposed to advanced glycosylation end products. *Kidney Int* **48**: 111–117.

Twigg SM, Cao Z, MCLennan SV, Burns WC, Brammar G, Forbes JM, Cooper ME (2002a). Renal connective tissue growth factor induction in experimental diabetes is prevented by aminoguanidine. *Endocrinology* **143**: 4907–4915.

Twigg SM, Joly AH, Chen MM, Tsubaki J, Kim HS, Hwa V *et al.* (2002b). Connective tissue growth factor/IGF-binding protein-related protein-2 is a mediator in the induction of fibronectin by advanced glycosylation end-products in human dermal fibroblasts. *Endocrinology* **143**: 1260–1269.

Vaitkevicius PV, Lane M, Spurgeon H, Ingram DK, Roth GS, Egan JJ *et al.* (2001). A cross-link breaker has sustained effects on arterial and ventricular properties in older rhesus monkeys. *Proc Natl Acad Sci USA* **98**: 1171–1175.

Vasan S, Zhang X, Zhang X, Kapurniotu A, Bernhagen J, Teichberg S *et al.* (1996). An agent cleaving glucose-derived protein crosslinks *in vitro* and *in vivo*. *Nature* **382**: 275–278.

Wang LL, Liu HY, Wang RH, Cui H, Li S (2004). Screening breaker of advanced-glycation end-product cross-links by enzyme-linked immunosorbent assay method *in vitro*. *Chin J Pharmacol Toxicol* **18**: 228–232.

Whittaker P, Kloner RA, Boughner DR, Pickering JG (1994). Quantitative assessment of myocardial collagen with picrosirius red staining and circularly polarized light. *Basic Res Cardiol* **89**: 397–410.

Wolffenbuttel BH, Boulanger CM, Crijns FR, Huijberts MS, Poitevin P, Swennen GN *et al.* (1998). Breakers of advanced glycation end products restore large artery properties in experimental diabetes. *Proc Natl Acad Sci USA* **95**: 4630–4634.

Yan SD, Schmidt AM, Anderson GM, Zhang J, Brett J, Zou YS *et al.* (1994). Enhanced cellular oxidant stress by the interaction of advanced glycation end products with their receptors/binding proteins. *J Biol Chem* **269**: 9889–9897.

Yin FC, Guzman PA, Brin KP, Maughan WL, Brinker JA, Traill TA *et al.* (1983). Effect of nitroprusside on hydraulic vascular loads on the right and left ventricle of patients with heart failure. *Circulation* **67**: 1330–1339.

Zhou G, Li C, Cai L (2004). Advanced glycation end-products induce connective tissue growth factor-mediated renal fibrosis predominantly through transforming growth factor beta-independent pathway. *Am J Pathol* **165**: 2033–2043.

Zhou Z, Wang K, Penn MS, Marso SP, Lauer MA, Forudi F *et al.* (2003). Receptor for AGE (RAGE) mediates neointimal formation in response to arterial injury. *Circulation* **107**: 2238–2243.

Zieman SJ, Kass DA (2004). Advanced glycation endproduct cross-linking in the cardiovascular system: potential therapeutic target for cardiovascular disease. *Drugs* **64**: 459–470.